

Series analysis of the 3-state Potts model in (2+1) dimensions

This article has been downloaded from IOPscience. Please scroll down to see the full text article.

1992 J. Phys. A: Math. Gen. 25 1821

(<http://iopscience.iop.org/0305-4470/25/7/023>)

View [the table of contents for this issue](#), or go to the [journal homepage](#) for more

Download details:

IP Address: 171.66.16.62

The article was downloaded on 01/06/2010 at 18:14

Please note that [terms and conditions apply](#).

Series analysis of the 3-state Potts model in (2+1) dimensions

C J Hamer, J Oitmaa and Zheng Weihong

School of Physics, The University of New South Wales, PO Box 1, Kensington, NSW 2033, Australia

Received 12 June 1991

Abstract. Both high-temperature and low-temperature series are used to locate and characterize the first-order transition in the 3-state Potts model in (2+1) dimensions on both square and triangular lattices. Estimates are presented for the vacuum energy, latent heat, magnetization, susceptibility and mass gap at the transition. The spontaneous magnetization and latent heat appear to display an 'approximate universality' at this weak first-order transition.

1. Introduction

There has recently been a resurgence of interest in the three-dimensional 3-state Potts model. It is commonly thought to undergo a weak first-order phase transition, but this was brought into some question when the APE collaboration (Bacilieri *et al* 1988) performed a large Monte Carlo simulation of the SU(3) gauge theory at finite temperature, which ought to be in the same universality class as the Potts model. They found a large correlation length, increasing with lattice size, which appeared to indicate a second-order transition. The Columbia group (Brown *et al* 1988), on the other hand, found that the SU(3) transition was indeed first-order.

This minor controversy was enough to trigger a renewed appraisal of the Potts model. Several Monte Carlo treatments have recently appeared (Fukugita and Okawa 1989, Gavai *et al* 1989, Gupta *et al* 1990, Fukugita *et al* 1990, Alves *et al* 1991, Bonfim 1991), which have concentrated particularly on the correlation length, and the finite-size scaling behaviour of the system. They conclude that the correlation length remains finite though large at the transition point, so that the transition is confirmed as being first-order.

In the present work we use series methods to study the quantum Hamiltonian version of the 3-state Potts model in (2 + 1) dimensions. Series have previously been calculated for the Euclidean version of the model by Ditzian and Oitmaa (1974), Enting (1974), Straley (1974), Kim and Joseph (1975) and Miyashita *et al* (1979), but they reached no definite conclusion as to the order of the transition. A first-order transition is difficult to characterize, or even detect, using either high-temperature (HT) series or low-temperature (LT) series alone. It is better to use both high-temperature and low-temperature series simultaneously to locate the transition, by means of a 'pincer' strategy. This technique was recently used by Guttmann and Enting (1990) for the Euclidean model, and we use it again here. The only previous study of the

Hamiltonian model which we know of is that of Hamer *et al* (1990, hereafter referred to as I), which used high-temperature series combined with a Monte Carlo simulation to locate the transition.

The methods we use are reviewed briefly in section 2, and the series analysis is presented in section 3. Our conclusions are summarized in section 4. Estimates are given for the transition point, the spontaneous magnetization, the latent heat, and the mass gap at the transition. Expressed in percentage terms, the spontaneous magnetization and the latent heat appear to be remarkably similar for the Hamiltonian model on the square lattice and the triangular lattice, and for the Euclidean model. We speculate that this 'approximate universality' at a first-order transition may be connected with the weakness of the transition, so that the correlation length at the transition, though finite, is very large, and washes out the microscopic details of the interaction. The behaviour of the mass gap is also discussed.

2. Method

High-temperature series expansions for the $(2+1)$ -dimensional 3-states Potts model have been obtained previously in reference I. The high-temperature form of the Hamiltonian is (Mittag and Stephen 1971, Solyom 1981)

$$H = -2 \sum_i \cos\left(\frac{2\pi}{3} L_i\right) - \lambda \sum_{\langle ij \rangle} (R_i^+ R_j^- + R_i^- R_j^+) \quad (2.1)$$

where i labels the sites on a two-dimensional spatial lattice, $\langle ij \rangle$ denotes nearest-neighbour pairs of sites, and λ is the coupling (corresponding to the inverse temperature in the Euclidean formulation).

In this paper, we derive the complementary low-temperature series expansion for the model, where the corresponding Hamiltonian is

$$H' = -2 \sum_{\langle ij \rangle} \cos\left[\frac{2\pi}{3}(L_i - L_j)\right] - \lambda' \sum_i (R_i^+ + R_i^-) \quad (2.2)$$

where L_i and R_i^\pm are operators at each site, which in a basis of eigenstates of L_i obey the rules

$$L_i |l_i\rangle = l_i |l_i\rangle \quad l_i = 0, 1, 2 \quad (2.3)$$

and

$$R_i^\pm |l_i\rangle = |(l_i \pm 1) \bmod 3\rangle \quad (2.4)$$

so that R_i^\pm are raising and lowering operators for the spin l_i , modulo 3. The two versions of the Hamiltonian are related by

$$H(\lambda) = \frac{1}{\lambda'} H'(\lambda') \quad \lambda = 1/\lambda'. \quad (2.5)$$

For the low-temperature version, the magnetic field term to be added to the Hamiltonian (2.2) is taken as

$$H_M = h \sum_i \cos\left(\frac{2\pi}{3} L_i\right) \quad (2.6)$$

and the spontaneous magnetization and susceptibility are defined as

$$\begin{aligned} M_0 &= \frac{1}{N} \left. \frac{\partial E_0(h, \lambda')}{\partial h} \right|_{h=0} \\ \chi &= -\frac{1}{N} \left. \frac{\partial^2 E_0(h, \lambda')}{\partial^2 h} \right|_{h=0} \end{aligned} \quad (2.7)$$

where N is the number of lattice sites.

There are two sectors of excited states in the model, symmetric and antisymmetric, respectively, under a spin-parity transformation. The lowest excited state in each sector is a single site excitation, in both the HT and LT phases. In the high-temperature series expansion the two states have the same eigenvalues F^S and F^A , but in the low-temperature expansion the two states differ, except in the limit of $\lambda' = 0$.

The low-temperature series expansions for the model have been obtained using Nickel's cluster expansion method (1980). The necessary techniques were reviewed recently by He *et al* (1990), and will not be repeated here. In these calculations, the first term in (2.2), $-2 \sum_{\langle ij \rangle} \cos[(2\pi/3)(L_i - L_j)]$, is taken as the unperturbed Hamiltonian, diagonal in the basis of eigenvectors of L_i , while the second term, $-\lambda' \sum_i (R_i^+ + R_i^-)$, then acts as a perturbation which 'flips' the spin at site i .

3. Series analysis

Series have been calculated for the ground-state energy per site E_0/N , the magnetization M_0 , the susceptibility χ , and the symmetric and antisymmetric lowest-lying excited state eigenvalues F^S , F^A on both the square lattice and the triangular lattice. For the ground-state energy and its derivatives, a list of 502 linked clusters (up to 10 sites) for the square lattice or 2129 linked clusters (up to 10 sites) for the triangular lattice was required. The energy gap involved 528 clusters (up to 9 sites) for the square lattice or 1480 clusters (up to 9 sites) for the triangular lattice, both linked and unlinked. The calculation occupied some 120 hours of CPU time for the square lattice and 400 hours of CPU time for the triangular lattice on an IBM3090. The resulting series for this model on the square and triangular lattices are listed in tables 1 and 2.

The analysis of these series was carried out as follows. Firstly, we have performed a standard Dlog Padé analysis (Guttman 1989) of the series for the derivative of the ground-state energy per site, magnetization, susceptibility, and mass gap, as for a model with a normal second-order phase transition. The results are exhibited in table 4 together with the those from the high-temperature expansion series obtained in reference I. The Dlog Padé analysis did not give a very good result for the case of the susceptibility series on the triangular lattice, but a significant improvement was gained by using second-order confluent differential approximants (Guttman 1989). The results are shown in table 3. From this table, we estimate that the apparent critical point lies at $\lambda_c^L = 4.080(8)$ (that is, $\lambda_c^L = 0.2451(5)$), with critical index

Table 1. Low-temperature series coefficients for the ground-state energy per site E_0/N , the spontaneous magnetization M_0 , and the susceptibility χ . Coefficients of λ^n are listed for the square and triangular lattices.

n	E_0/N	M_0	χ
Square lattice			
0	-4	1	0
1	0	0	0
2	-1.66666666667E-01	-2.08333333333E-02	5.20833333333E-03
3	-1.38888888889E-02	-3.47222222222E-03	1.30208333333E-03
4	-1.047178130511E-03	-7.443756823717E-04	5.728376190276E-04
5	-2.893518518519E-04	-2.732767489712E-04	2.618902177641E-04
6	-6.210846249794E-05	-7.362018501286E-05	9.137088662052E-05
7	-1.184658489194E-05	-2.096679943791E-05	3.453547666403E-05
8	-3.342271499429E-06	-7.015409645460E-06	1.360355435898E-05
9	-9.705310401687E-07	-2.319141497062E-06	5.249748958030E-06
10	-2.773825591688E-07	-7.786375209009E-07	2.041457638106E-06
11	-8.175438578586E-08	-2.627731525926E-07	7.829374078637E-07
12	-2.386217812185E-08	-8.791220529922E-08	2.969312377822E-07
13	-7.208029941710E-09	-3.003007170112E-08	1.134566937906E-07
14	-2.285537067890E-09	-1.046167725701E-08	4.352721704361E-08
15	-7.315630086485E-10	-3.657315605767E-09	1.666029175193E-08
16	-2.339630891559E-10	-1.279468570129E-09	6.357310162579E-09
17	-7.530587146052E-11	-4.487654316849E-10	2.420730778299E-09
18	-2.454983233539E-11	-1.583161525936E-10	9.221080408443E-10
19	-8.131763607716E-12	-5.627251031485E-11	3.518097956941E-10
20	-2.722484786373E-12	-2.010041160867E-11	1.342767768690E-10
21	-9.149097359207E-13	-7.193960475398E-12	5.120722886428E-11
Triangular lattice			
0	-6	1	0
1	0	0	0
2	-1.11111111111E-01	-9.259259259259E-03	1.543209876543E-03
3	-6.172839506173E-03	-1.028806584362E-03	2.572016460905E-04
4	-2.556428482354E-04	-1.220680429435E-04	6.170451925987E-05
5	-4.191434232586E-05	-2.768886856678E-05	1.770986807567E-05
6	-6.458128005391E-06	-5.079715430319E-06	4.119749751020E-06
7	-9.010574368989E-07	-9.925286106656E-07	1.042079278821E-06
8	-1.652302223543E-07	-2.153500021045E-07	2.654289694439E-07
9	-2.909944866023E-08	-4.456285870763E-08	6.477704862943E-08
10	-5.162754579363E-09	-9.478970528428E-09	1.607480225699E-08
11	-9.980113078545E-10	-2.079451276240E-09	3.991144555161E-09
12	-1.935840239499E-10	-4.545559862194E-10	9.823286089554E-10
13	-3.807532677699E-11	-1.005485265567E-10	2.424609757153E-10
14	-7.71323333150E-12	-2.249641670730E-11	5.982034087154E-11
15	-1.578311537009E-12	-5.052763883443E-12	1.473125528589E-11
16	-3.269331702976E-13	-1.142813355451E-12	3.630014081219E-12
17	-6.869860787491E-14	-2.600930589549E-13	8.944146265777E-13
18	-1.453846335970E-14	-5.942336637995E-14	2.202469779771E-13
19	-3.109079362475E-15	-1.363050543491E-14	5.422399653255E-14
20	-6.693093953533E-16	-3.137976150000E-15	1.334593086236E-14
21	-1.450503323791E-16	-7.246814315764E-16	3.283927162224E-15

$\gamma = -1.06(3)$, which agrees with that obtained by the ratio method (Guttman 1989) which predicts $\lambda_c^L = 4.073(13)$.

It can be seen that the apparent second-order critical points derived from the magnetization, susceptibility, and mass gap series are in almost perfect agreement

Table 2. Low-temperature series coefficients for the symmetric energy gap F^S and antisymmetric energy gap F^A . Coefficients of λ^n are listed for square and triangular lattices.

n	Square lattice		Triangular lattice	
	F^S	F^A	F^S	F^A
0	12	12	18	18
1	-1	-1	-1	-1
2	-5.55555555556E-01	-5.00000000000E-01	-2.44444444444E-01	-2.22222222222E-01
3	-1.327160493827E-01	-1.52777777777E-01	-4.358024691358E-02	-4.012345679012E-02
4	5.616794042720E-03	-7.594797178131E-03	-4.062227210375E-03	-4.748098266617E-03
5	1.201465096784E-02	5.947788065844E-03	-5.764079408627E-04	-1.173934994665E-03
6	-3.020170924430E-03	-4.295823172281E-05	-1.849732256247E-04	-2.421175630984E-04
7	-2.969683954259E-03	-2.110541869481E-03	4.886027857570E-08	-3.851997646933E-05
8	-6.221445613164E-04	-1.020071040392E-03	-3.246897559863E-06	-7.347623244466E-06
9	5.172309644717E-04	-2.605878683522E-06	-2.400733398541E-07	-1.546025274667E-06
10	2.272261494410E-04	1.822465349205E-04	-2.847105578792E-07	-2.975082333044E-07
11	-6.365824021242E-05	4.979655653784E-05	-2.026842183202E-08	-5.812433806549E-08
12	-7.151910312984E-05	-2.764031776127E-05	-1.094501447075E-08	-1.239740502751E-08
13	-3.370840213499E-06	-2.173638357627E-05	-1.120695267999E-09	-2.797693380846E-09
14	1.684237806237E-05	-1.224526515136E-06	-4.903372635847E-10	-6.706575559947E-10
15	4.835502699553E-06	4.641197024298E-06	-7.899505132628E-11	-1.680047947013E-10
16	-3.014466780191E-06	1.846256775656E-06	-1.573722930150E-11	-4.102466798619E-11
17	-2.050795956432E-06	-5.147328268003E-07	-3.774796793964E-12	-9.333227178958E-12

with one another in every case, so we assume henceforth that they are the same for each different quantity. Table 4 also shows that the apparent critical indices appear to be universal between the square and the triangular lattice. However, the critical points derived from the HT and LT series, λ_c^H and λ_c^L respectively, ‘cross over’ each other by a small but significant amount, of order 2%, which is several times bigger than our expected error. If the transition were really second-order, the two results should agree. This provides the first signal that the system actually undergoes a first-order transition, located somewhere in between the two pseudo-critical points λ_c^H and λ_c^L .

Next, we have used the high-temperature and low-temperature series directly to extrapolate each thermodynamic quantity in towards the transition point, starting from the high- and low-temperature limits respectively. An obvious way to do this would be to calculate Padé approximants to each series; but Padé approximants are best suited to functions whose only singularities are simple poles, whereas the functions we are interested in have cuts at the spinodal pseudo-critical points, characterized by the parameters given in table 4, only a little way beyond the first-order transition point. It seems better, therefore, to use differential approximants (Guttman 1989) rather than Padé approximants. A first-order inhomogeneous differential approximant, for example, represents a function $f(z)$ by the differential equation,

$$Q_1(z)zf'(z) + Q_0(z)f(z) = P(z) \tag{3.1}$$

where $P(z)$, $Q_0(z)$ and $Q_1(z)$ are polynomials. The equation allows solutions of the form

$$f(z) \sim A(z)|z - z_0|^\alpha + B(z) \tag{3.2}$$

near a singular point z_0 , which is well suited to our requirements. At a given order, one determines the polynomials $P(z)$, $Q_0(z)$ and $Q_1(z)$ by matching the series expansions

Table 3. Table of second-order confluent differential approximants to the LT susceptibility series on the triangular lattice. Estimates of the apparent second-order critical point λ_c^L and index γ (in brackets) are shown, which come from the $[L/N + \Lambda; N]$, $\Lambda = -1, 0, 1$ approximants, in the notation of Guttman (1989).

	Λ	$N = 2$	$N = 3$	$N = 4$	$N = 5$
$L = 1$	-1	4.00927	4.03915	4.07564	4.08288
		(-0.9596)	(-0.8489)	(-1.0344)	(-1.0609)
	0	4.00074	4.07848	4.08422	4.07453
		(-0.9696)	(-1.0457)	(-1.0546)	(-1.0403)
	1	4.08399	4.03358 ^a	4.06588 ^a	
		(-1.0665)	(-1.6799)	(-1.0009)	
$L = 2$	-1	3.95136	4.00624	4.06981	4.08212
		(-0.9470)	(-0.9041)	(-1.0216)	(-1.0594)
	0	3.95119 ^a	4.07596	4.07641	4.07392
		(-0.9731)	(-1.0355)	(-1.0463)	(-1.0383)
	1	4.08373	4.07632	4.05050 ^a	
		(-1.0674)	(-1.0462)	(-0.7725)	
$L = 3$	-1	4.03001	4.04554	4.09028	4.08061 ^a
		(-1.0094)	(-0.9844)	(-1.0714)	(-1.0797)
	0	4.05348	4.24691	4.08127	
		(-1.0000)	(1.2158)	(-1.0713)	
	1	4.07829	4.07643	4.07768	
		(-1.0468)	(-1.0464)	(-1.0576)	
$L = 4$	-1	3.96874	4.15669	4.02009 ^a	4.07872 ^a
		(-1.0105)	(-1.1780)	(-0.6327)	(-1.0630)
	0	4.05038	4.09613	4.08410 ^a	
		(-0.9977)	(-1.0732)	(-1.1148)	
	1	4.08012	4.08012		
		(-1.0572)	(-1.0558)		

^a Estimates defective.

on either side of (3.1) up to the given order. Then the corresponding approximant to $f(z)$ may be found by numerical integration of (3.1). This sort of procedure has been discussed previously by Hunter and Baker (1979) and Liu and Fisher (1989), and was also used by Guttman and Enting (1990) in their recent series analysis.

Figures 1 and 2 show the results for the ground-state energy per site (figure 1 displays results for a number of different approximants). It can be seen that the high-temperature and low-temperature extrapolations cross each other at a distinct angle, which is again characteristic of a first-order transition. The transition point where the two lines cross is found to be

$$\begin{aligned} \lambda_c &= 0.3806(6) && \text{(square lattice)} \\ \lambda_c &= 0.2466(2) && \text{(triangular lattice)}. \end{aligned} \tag{3.3}$$

Table 4. Estimates of singularity parameters, for the pseudo second-order phase transitions, obtained by Dlog Padé approximants and confluent differential approximants to the series given in reference I and tables 1 and 2. Both unbiased and biased estimates are listed.

	E'_0/N	M_0	χ	F^S	F^A	
Dlog Padé to the HT series on the square lattice						
Unbiased estimates	λ_c^H		0.388(2)	0.388(3)		
	Index		-0.97(2)	0.54(2)		
Biased at $\lambda_c^H = 0.388(2)$	Index		-0.97(2)	0.535(12)		
Dlog Padé to the LT series on the square lattice						
Unbiased estimates	λ_c^L	0.379(4)	0.3784(2)	0.3781(7)	0.379(5)	0.380(9)
	Index	0.19(8)	0.197(2)	-1.15(5)	0.57(5)	0.37(8)
Biased at $\lambda_c^L = 0.3784(2)$	Index	0.19(2)	0.1971(10)	-1.125(10)	0.571(8)	0.41(3)
Dlog Padé to the HT series on the triangular lattice						
Unbiased estimates	λ_c^H		0.2487(10)	0.249(1)		
	Index		-0.90(4)	0.50(3)		
Biased at $\lambda_c^H = 0.2487(10)$	Index		-0.90(4)	0.49(2)		
Dlog Padé to LT series on the triangular lattice						
Unbiased estimates	λ_c^L	0.243(3)	0.244(2)	0.244(2)	0.2475(30)	0.243(5)
	Index	0.25(7)	0.20(2)	-1.15(10)	0.48(10)	0.39(10)
Biased at $\lambda_c^L = 0.2451(5)$	Index	0.196(15)	0.18(2) ^a	-1.04(6)	0.57(4)	0.37(2)
Confluent differential approximant to the LT series on the triangular lattice						
Unbiased estimates	λ_c^L		0.247(2)	0.2451(5)		
	Index		0.35(15)	-1.06(3)		
Biased at $\lambda_c^L = 0.2451(5)$	Index		-0.185(15)	-1.06(3)		

^a Estimates defective.

The remaining functions, namely the magnetization, the susceptibility and the mass gap (and also the derivative of the low-temperature ground-state energy), vary rapidly near the transition point because of the nearby pseudo-critical point. It is useful therefore to 'smooth' each of these functions before making the extrapolations (Liu and Fisher 1989), by calculating approximants to the series for $(1 - \lambda/\lambda_c^{(s)})^{-\nu} f(\lambda)$ rather than $f(\lambda)$ itself, where $\lambda_c^{(s)}$ and ν are the pseudo-critical point and critical index, respectively.

The results are given in tables 5 and 6, and in figures 3-6. The errors arise mainly from the uncertainties in the critical parameters λ_c , $\lambda_c^{(s)}$ and ν in each case. At the transition point given by (3.3) we estimate that:

(i) The derivative of the ground-state energy is discontinuous at this point, as illustrated in figure 3,

$$\frac{1}{N} \frac{dE_0}{d\lambda} = \begin{cases} -0.75(2) & \lambda \rightarrow \lambda_c^- \\ -1.17(10) & \lambda \rightarrow \lambda_c^+ \end{cases} \quad (\text{square lattice}) \quad (3.4)$$

$$\frac{1}{N} \frac{dE_0}{d\lambda} = \begin{cases} -0.943(5) & \lambda \rightarrow \lambda_c^- \\ -1.68(9) & \lambda \rightarrow \lambda_c^+ \end{cases} \quad (\text{triangular lattice}). \quad (3.5)$$

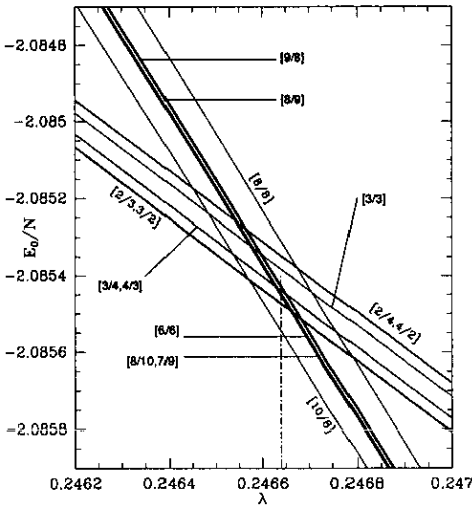


Figure 1. Graph of the ground state energy per site E_0/N against λ for the triangular lattice. Integrated Dlog Padé approximants to both the HT series and LT series are labelled by order $[N/M]$. The phase transition is expected at $\lambda_c = 0.24664(20)$ marked by the broken vertical line.

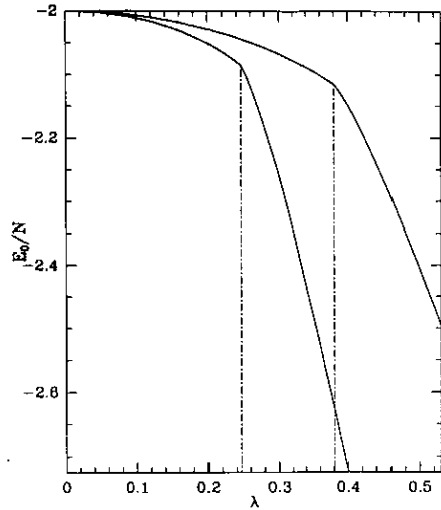


Figure 2. Graph of the ground state energy per site E_0/N against λ for both the square lattice and the triangular lattice. The broken vertical lines mark the expected phase transitions.

Thus we estimate the discontinuity or ‘latent heat’ as

$$L \equiv \frac{1}{N} \left(\frac{\partial E_0}{\partial \lambda} \Big|_{\lambda=\lambda_c-} - \frac{\partial E_0}{\partial \lambda} \Big|_{\lambda=\lambda_c+} \right) = \begin{cases} 0.42(10) & \text{(square lattice)} \\ 0.74(9) & \text{(triangular lattice)}. \end{cases} \quad (3.6)$$

Some selected values for the ground-state energy and its derivative for the square lattice are also given as functions of coupling λ in tables 5 and 6, along with our previous Monte Carlo results (reference I). The series and Monte Carlo estimates are in good agreement.

(ii) The spontaneous magnetization is

$$M_0 = \begin{cases} 0.42(3) & \text{(square lattice)} \\ 0.42(2) & \text{(triangular lattice)} \end{cases} \quad (3.7)$$

i.e. 42% of the maximum possible value for both lattices. This agrees well with the Monte Carlo estimate (reference I) of 43(7)% for the square lattice.

(iii) The susceptibility shows a large discontinuity at λ_c for both lattices, as given in tables 5 and 6.

(iv) The symmetric mass gap at λ_c is found to be

$$F^S = \begin{cases} 0.36(4) & \lambda \rightarrow \lambda_c- \\ 0.32(4) & \lambda \rightarrow \lambda_c+ \end{cases} \quad \text{(square lattice)} \quad (3.8)$$

$$F^S = \begin{cases} 0.28(5) & \lambda \rightarrow \lambda_c- \\ 0.36(6) & \lambda \rightarrow \lambda_c+ \end{cases} \quad \text{(triangular lattice)}. \quad (3.9)$$

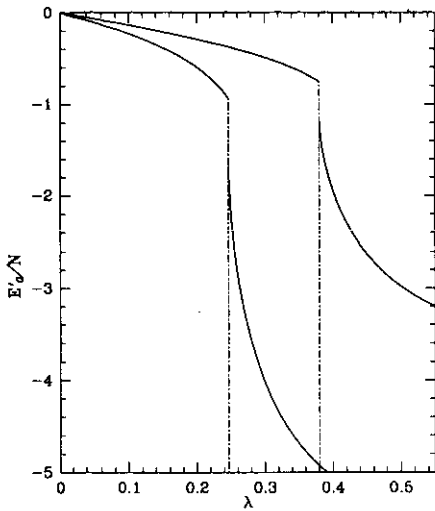


Figure 3. Graph of the derivative of the ground state energy per site, E'_0/N against λ for both the square lattice and the triangular lattice. The broken vertical lines mark the expected phase transitions.

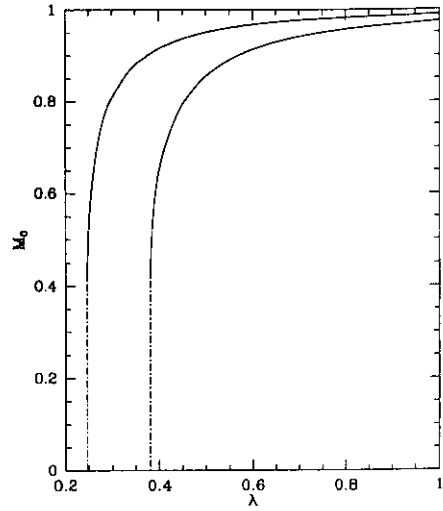


Figure 4. Graph of the spontaneous magnetization M_0 against λ for both the square lattice and the triangular lattice.

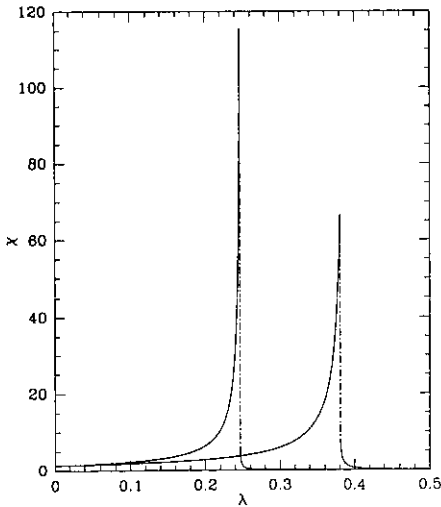


Figure 5. Graph of the susceptibility χ against λ for both the square and triangular lattices.

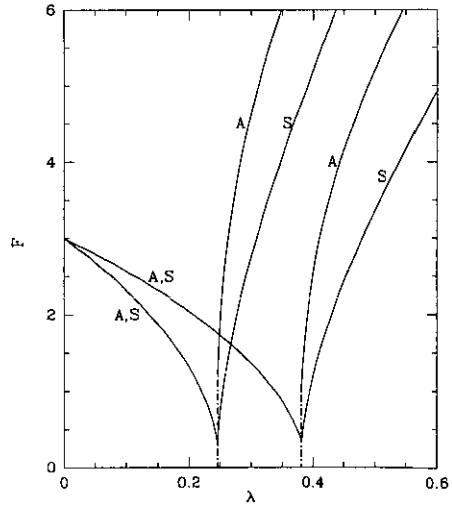


Figure 6. Graph of the symmetric and antisymmetric mass gap F^S and F^A against λ for both the square and triangular lattices.

In other words, the mass gap is small but finite at the transition point, as one would expect for a weak first-order transition, and our data are consistent, within errors, with the possibility that the symmetric mass gap, at least, is continuous from the low-temperature to the high-temperature phase. The antisymmetric mass gap, on the other hand, certainly seems to undergo a substantial discontinuity at the phase

Table 5. Values for the ground state energy per site E_0/N , the derivative of the ground-state energy per site $E'_0/N = 1/N(dE_0/d\lambda)$, the magnetization M_0 , the susceptibility χ , the symmetric energy gap F^S , and the antisymmetric energy gap F^A on the square lattice as a function of coupling λ estimated by integrated differential approximant to the HT series (for $\lambda \leq \lambda_{c-}$) or the LT series (for $\lambda \geq \lambda_{c+}$). Also shown are the results of ground-state energy per site E_0 from Monte Carlo simulation in the bulk limit of reference I.

λ	E_0/N	E_0/N by MC	E'_0/N	M_0	χ	F^S	F^A
0.05	-2.001682	-2.001682(3)	-0.067668	0	1.5374	2.7915	
0.10	-2.006812	-2.006815(7)	-0.138110	0	1.8119	2.5650	
0.15	-2.015564	-2.01555(2)	-0.212814(3)	0	2.2003	2.3172(4)	
0.20	-2.028200	-2.02820(3)	-0.29398(4)	0	2.7922(4)	2.0427(10)	
0.25	-2.045127(8)	-2.0451(1)	-0.3852(4)	0	3.805(3)	1.731(6)	
0.30	-2.06700(8)	-2.0670(5)	-0.493(2)	0	5.94(3)	1.36(1)	
0.35	-2.0949(2)	-2.094(1)	-0.633(8)	0	13.6(3)	0.87(2)	
0.375	-2.1117(4)	—	-0.73(2)	0	39(5)	0.49(3)	
λ_{c-}	-2.1157(6)	—	-0.75(2)	0	67(14)	0.36(4)	
λ_{c+}	-2.1157(3)	—	-1.17(10)	0.42(3)	8(3)	0.32(4)	1.0(2)
0.40	-2.1484(1)	-2.147(2)	-1.936(8)	0.6493(10)	0.588(10)	1.194(14)	2.55(9)
0.425	-2.202508(8)	—	-2.3522(8)	0.7424(1)	0.239(2)	1.872(10)	3.48(3)
0.45	-2.264904(3)	-2.2640(7)	-2.6235(2)	0.79460(5)	0.1430(2)	2.419(5)	4.152(15)
0.50	-2.405676	-2.4056(5)	-2.97724(2)	0.85533(1)	0.0741	3.348(2)	5.206(6)
0.55	-2.560530	—	-3.201883	0.890504(7)	0.0475	4.1686(10)	6.087(2)
0.60	-2.724724	—	-3.357013	0.913519(5)	0.0337	4.9314(4)	6.8840(5)
0.70	-3.071238	—	-3.554623	0.941516(4)	0.0201	6.3612	8.3498
0.80	-3.433049	—	-3.672353	0.957559(3)	0.0135	7.7186	9.7242

transition, as shown in tables 5 and 6 (recall that F^S and F^A are identical in the HT phase).

4. Summary and discussion

High-temperature and low-temperature series expansions have been obtained for the model on both the square and triangular lattices, and extrapolated to the transition point using integrated differential approximants. The transition point has been taken as the point where the high-temperature and low-temperature extrapolations for the ground-state energy cross over, and our result is:

$$\lambda_c = \begin{cases} 0.3806(6) & \text{(square lattice)} \\ 0.2466(2) & \text{(triangular lattice)}. \end{cases} \quad (4.1)$$

This agrees with the previous Monte Carlo estimate (reference I) $\lambda_c = 0.379(3)$ for the square lattice.

The spontaneous magnetization at λ_c is estimated as

$$M_0 = \begin{cases} 0.42(3) & \text{(square lattice)} \\ 0.42(2) & \text{(triangular lattice)} \end{cases} \quad (4.2)$$

Table 6. Values for the ground-state energy per site E_0/N , the derivative of the ground-state energy per site E'_0/N , the magnetization M_0 , the susceptibility χ , the symmetric energy gap F^S , and the antisymmetric energy gap F^A on the triangular lattice as a function of coupling λ estimated by integrated differential approximant to the HT series (for $\lambda \leq \lambda_c^-$) or the LT series (for $\lambda \geq \lambda_c^+$).

λ	E_0/N	E'_0/N	M_0	χ	F^S	F^A
0.05	-2.002613	-0.107059	0	1.6650	2.6809	
0.10	-2.011011	-0.23261(5)	0	2.2114	2.3147(2)	
0.15	-2.026361	-0.38779(8)	0	3.2848(6)	1.8783(6)	
0.20	-2.05069(2)	-0.600(2)	0	6.410(8)	1.311(5)	
0.225	-2.06743(5)	-0.752(3)	0	12.50(8)	0.91(2)	
λ_c^-	-2.0854(4)	-0.943(6)	0	115(15)	0.28(5)	
λ_c^+	-2.0854(2)	-1.68(9)	0.42(2)	4(1)	0.36(6)	1.2(3)
0.25	-2.0926(2)	-2.17(4)	0.536(8)	1.1(2)	0.67(5)	1.86(8)
0.275	-2.16586(1)	-3.4213(6)	0.7366(2)	0.1512(10)	1.93(2)	3.65(3)
0.30	-2.259465	-4.01731(6)	0.80926(2)	0.0749(4)	2.750(4)	4.627(10)
0.35	-2.478861	-4.683488(4)	0.880244(3)	0.0340(2)	4.0647(8)	6.0535(15)
0.40	-2.723025	-5.051490	0.916031	0.0205	5.2084(4)	7.2313(5)
0.45	-2.981757	-5.281409	0.937385	0.0141	6.2714(2)	8.3059(2)
0.50	-3.249928	-5.435872	0.951343	0.0103	7.2885	9.3265

which again agrees well with the Monte Carlo estimate (reference I) $M_0 = 0.43(7)$ for the square lattice. It is also remarkably similar to the Euclidean model result, where Monte Carlo studies (Knak Jensen and Mouritsen 1979, Wilson and Vause 1987, Gavai *et al* 1989) find a spontaneous magnetization very close to 40%, while the series analysis of Guttman and Enting (1990) finds $M_0 = 0.365(30)$.

The 'latent heat' was estimated from the discontinuity in the derivative of the ground-state energy as

$$L = \begin{cases} 0.42(10) & \text{or } 10(3)\% & \text{(square lattice)} \\ 0.74(9) & \text{or } 12(2)\% & \text{(triangular lattice)} \end{cases} \quad (4.3)$$

where the percentages are calculated relative to the maximum possible absolute value in each case. In the Euclidean model case, a series analysis (Guttman and Enting 1990) finds 14(3)% for the latent heat, while Monte Carlo simulations (Knak Jensen and Mouritsen 1979, Gavai *et al* 1989, Alves *et al* 1991) give a figure very close to 8%. In our case, we found that the series estimate of the latent heat was quite sensitive to the method of extrapolation used (particularly the 'smoothing' of the derivative function discussed in section 3). A similar effect might explain the discrepancy between the series and Monte Carlo estimates in the Euclidean case.

The various results for the latent heat and the spontaneous magnetization, all expressed as percentages, are listed for comparison in table 7. The striking feature is how similar the results are, firstly for the square and triangular lattices in the Hamiltonian formulation, and secondly for the Hamiltonian and Euclidean formulations. Apart from the discrepancy in latent heat referred to above, the results look very much the same. There appears to be at least an approximate 'universality' between the different

cases. Now universality is normally expected to hold only at second-order transitions, where the correlation length scale goes to infinity, so that local details of the lattice structure become unimportant. It appears that an approximate form of universality may hold also for a weak first-order transition such as the present one, at which the correlation length, though finite, is very large (of order ten lattice units).

Table 7. A comparison of the results obtained in the present work with some previous calculations, for the spontaneous magnetization and latent heat. Both quantities are expressed as percentages of their maximum possible values. (MC = Monte Carlo; s = series.)

		Spontaneous magnetization (%)	Latent heat (%)
Hamiltonian model, square lattice			
MC	Hamer <i>et al</i> 1990	43(7)	
s	This work	42(3)	10.5(2.5)
Hamiltonian model, triangular lattice			
s	This work	42(2)	12(2)
Euclidean model, cubic lattice			
s	Guttman and Enting 1990	36.5(3.0)	14(3)
MC	Gavai <i>et al</i> 1989	39.5(5)	8.0(4)
MC	Alves <i>et al</i> 1991		8.03(3)

Finally, some estimates were obtained of the mass gaps in the even (S) and odd (A) spin-parity sectors, as follows:

$$F^S = \begin{cases} 0.36(4) & \lambda \rightarrow \lambda_{c-} \\ 0.32(4) & \lambda \rightarrow \lambda_{c+} \end{cases} \quad (4.4)$$

$$F^A = \begin{cases} 0.36(4) & \lambda \rightarrow \lambda_{c-} \\ 1.0(2) & \lambda \rightarrow \lambda_{c+} \end{cases} \quad (4.5)$$

for square lattice, and

$$F^S = \begin{cases} 0.28(5) & \lambda \rightarrow \lambda_{c-} \\ 0.36(6) & \lambda \rightarrow \lambda_{c+} \end{cases} \quad (4.6)$$

$$F^A = \begin{cases} 0.28(5) & \lambda \rightarrow \lambda_{c-} \\ 1.2(3) & \lambda \rightarrow \lambda_{c+} \end{cases} \quad (4.7)$$

for triangular lattice. Thus the mass gap remains finite, though small, as one expects at a first-order transition. Euclidean Monte Carlo studies (Gavai *et al* 1989, Fukugita *et al* 1990) find a mass gap or inverse correlation length of about 0.1. Fukugita *et al* (1990) claim evidence of a small jump discontinuity in the mass gap at the transition, of order 15% of the total gap. Our accuracy is not sufficient to determine whether such a jump occurs or not; the high- and low-temperature extrapolations certainly end up very close to each other for the symmetric gap (equations (4.4) and (4.6)), although there is a substantial jump in the antisymmetric gap (equations (4.5) and (4.7)).

One would like to compare the sizes of the mass gaps in the Hamiltonian and Euclidean formulations, but unfortunately we have no absolute scale of comparison in the Hamiltonian case. The quantum Hamiltonian can always be rescaled by multiplication with an arbitrary constant. In studies of conformal invariance (von Gehlen *et al* 1986), this constant is fixed by setting the 'speed of light' in the model equal to unity, but that requires a study of the dispersion relations in the model, which we have not performed.

5. Acknowledgment

This work forms parts of a research project supported by a grant from the Australian Research Council.

References

- Alves N A, Berg B A and Villanova R 1991 *Phys. Rev. B* **43** 5846
 Bacilieri P *et al* 1988 *Phys. Rev. Lett.* **61** 1545
 Bonfim O F de A 1991 *J. Stat. Phys.* **62** 105
 Brown F R, Christ N H, Deng Y, Gao M and Woch T J 1988 *Phys. Rev. Lett.* **61** 2058
 Ditzian R V and Oitmaa J 1974 *J. Phys. A: Math. Gen.* **7** L61
 Enting I G 1974 *J. Phys. A: Math. Gen.* **7** 1617
 Fukugita M and Okawa M 1989 *Phys. Rev. Lett.* **63** 13
 Fukugita M, Mino H, Okawa M and Ukawa A 1990 *J. Stat. Phys.* **59** 1397
 Gavai R V, Karsch F and Petersson B 1989 *Nucl. Phys. B* **322** 738
 Gupta S, Irbäck A, Petersson B, Gavai R V and Karsch F 1990 *Nucl. Phys. B* **329** 263
 Guttman A J 1989 *Phase Transitions and Critical Phenomena* vol 13, ed C Domb and J Lebowitz (New York: Academic)
 Guttman A J and Enting I G 1990 *Nucl. Phys. B (Proc. Suppl.)* **17** 328
 Hamer C J, Aydin M, Oitmaa J and He H X 1990 *J. Phys. A: Math. Gen.* **23** 4025
 He H-X, Hamer C J and Oitmaa J 1990 *J. Phys. A: Math. Gen.* **23** 1775
 Hunter D L and Baker G A Jr 1979 *Phys. Rev. B* **19** 3808
 Kim D and Joseph R I 1975 *J. Phys. A: Math. Gen.* **8** 891
 Knak Jensen S J and Mouritsen O G 1979 *Phys. Rev. Lett.* **43** 1736
 Liu A J and Fisher M E 1989 *Physica* **156A** 35
 Mittag L and Stephen M J 1971 *J. Math. Phys.* **12** 441
 Miyashita S, Betts D D and Elliott C J 1979 *J. Phys. A: Math. Gen.* **12** 1605
 Nickel B G 1980 unpublished
 Solyom J 1981 *Phys. Rev. B* **24** 230
 Straley J P 1974 *J. Phys. A: Math. Gen.* **7** 2173
 Svetitsky B and Yaffe L G 1982a *Nucl. Phys. B* **210** 423
 — 1982b *Phys. Rev. D* **26** 963
 von Gehlen G, Rittenberg V and Ruegg H 1986 *J. Phys. A: Math. Gen.* **19** 107
 Wilson W G and Vause C A 1987 *Phys. Rev. B* **36** 587